Journal of Simulation and Analysis of Novel Technologies in Mechanical Engineering
13 (2) (2021) 0025~0038
HTTP://JSME.IAUKHSH.AC.IR

Research article

Dynamic stability analysis of functionally graded Euler-Bernoulli nanobeams under a sequence of moving nanoparticle based on nonlocal elasticity theory

Rahman Khanahmadi[1*], Mohammad Hashemian[2], Mostafa Pirmoradian[2]

[1]*Mechanical Engineering group, Pardis College, Isfahan University of Technology, Isfahan 84156-83111, Iran*
[2]*Department of Mechanical Engineering, Khomeinishahr Branch, Islamic Azad University, Isfahan, 84175-119, Iran*

[*]rahmankh371@gmail.com

(Manuscript Received --- 10 Nov. 2021; Revised --- 22 Nov. 2021; Accepted ---09 Dec. 2021)

Abstract

This study investigates the dynamic stability of the Euler-Bernoulli functionally graded (FGM) nanobeam based on the nonlocal elasticity theory while considering surface effects. Nanoparticles pass over nanobeam sequentially with a constant velocity, and the nanoparticle inertia is also considered. A thermal gradient with constant temperature changes is applied to this nanobeam. The functionally graded nanobeam properties, including Young's modulus, density, surface residual stress, and surface modulus are taken by the power law. The classical equations of motion are obtained by applying the Hamilton's principle according to the energy method. The governing equations are extracted using nonlocal elasticity theory, and the surface effects are taken by Gurtin-Murdoch theory. The dynamic stability graphs will be presented on nanoparticle mass-velocity coordinates. This article investigated the small scale effect parameter, temperature changes, Pasternak environment shearing and elastic constants, and the volume fraction parameter in power law. The results show that increasing Pasternak foundation constants increase the functionally graded nanobeam stability, and increasing small scale parameter reduces its stability. Increasing nanobeam temperature shifts the functionally graded stability region of nanobeam towards faster nanoparticle velocity, which indicates a higher dynamic stability for the nanobeam.

Keywords: Dynamic stability, Nanobeam, FGM, Moving nanoparticle, Nonlocal elasticity theory.

1- Introduction

Due to the growing importance of nanotechnology and nanostructure applications, understanding their properties and mechanical behavior is very important. Nano-electro-mechanical-systems (NEMS) are very sensitive to external excitation. Therefore, in their production, there is a need for more information on nanobeam vibrational behavior and stability. At first, Mindlin [1] (using the strain gradient theory) and then Eringen [2] (using the nonlocal elasticity theory) were able to provide a more accurate analysis of structures compared to classical theories by taking the small scale effect. In classical theories, stress at one point results from strain at the same point, while in nonlocal

theories, stress at one point is a function of strain at all points of the system [3]. Peddieson et al. [4] used the nonlocal elasticity theory on nanostructure materials. Their study indicates that the nonlocal elasticity theory is applicable to nano-scale, but inapplicable to micro-electro-mechanical-system (MEMS). Ansari and Sahmani [5] investigated the bending and buckling of nanobeams while considering surface effects. The results show the difference between the behaviors of the nanobeam predicted by the classical and non-classical theories which depends on the value of the surface elastic constants. In addition, researchers in many of the studies [6-8] have used the nonlocal elasticity theory and the results illustrate that in static and dynamic analysis of nanobeams, nonlocal small scale parameter has noticeable effect.

A type of nanotube which is used for injecting drug into the body is a nano-mechanism that can be considered a beam problem with moving mass. In this condition, the drugs are the sequentially moving nanoparticles and the nanotube can be considered a nanobeam. Hashemi and Khaniki [9] investigated the dynamic of multiple nanobeam system under a moving nanoparticle. The results show that small scale effect plays a principal role in the value of the dynamical deflection. Simsek [10] investigated the single walled carbon nanotube vibration under action of a moving load based on nonlocal theory. The results illustrate that dynamic deflection of the nanotube increase with increase in the small scale parameter. This means that the local beam theory is not a suitable method for dynamic deflection since it is not an accurate approximation and the effects of nonlocal parameters depend on nanotube dimensional ratio. Kiani and Mehri [11] studied the nanotube structures under a moving nanoparticle using nonlocal beam theories. The results of this study and others [12-18] also signify the importance of using nonlocal theories, especially for movement of low-velocity nanoparticles over nanostructures.

Regarding their unique properties and advantages, including increased thermal resistance and lowered stress intensity factor, functionally graded materials are widely used in nanostructure systems. The properties of functionally graded materials making them useful to reaching high sensitivity design applications [19, 20]. Material scientists in the Sendai region of Japan proposed using FGM as materials with high thermal tolerance for the first time. Functionally graded materials are composite heterogeneous materials and their mechanical properties moderately and continuously change from one surface to another [21]. The properties of these materials are approximated based on exponential or power functions. Hossein-Hashemi and Nazemnejad [22] investigated the nonlinear free vibration of functionally graded nanobeams while considering surface effects. The results showed that increasing FG nanobeam dimensions reduced the effects of surface on natural frequency. Hossein-Hashemi et al. [23] also studied surface effects on free vibration of FG nanobeams using the nonlocal elasticity theory. The results show that as surface effects increase, the impact of nonlocal parameters decrease. Simsek [15] studied the FG Timoshenko beam vibration under a moving harmonic load. According to this study, using power law for expressing beam property plays an important role on the stresses of the beam. Ke et al. [24] investigated the size effect on dynamic stability of FG microbeams. Results show

that the size effect on the dynamic stability is important only when the thickness of beam has a similar value to the material length scale parameter. Rahmani and Pedram [25] analyzed the vibration of FG nanobeams based on nonlocal beam theory. According to the results, the impact of length scale parameter and the thickness to length ratio is very important in analyzing nanobeam vibrations.

The difference between the Euler-Bernoulli and Timoshenko theories is that in the Euler-Bernoulli beam theory (EBT), the cross section of each surface remains flat after deflection, and the rotation of cross section surface is neglected in beams that have low thickness [26]. In the Timoshenko beam theory (TBT), it is no longer assumed that the surface remains vertical after deflection and shear deformation is shown through surface angle variations [27]. In dynamic stability analysis, movements resulting from excitations are compared as being time dependent. In comparing of dynamic stability and forced vibration of system, analyzing forced vibration excitations appear as a somewhat heterogeneous term in governing equations, but in analysis of dynamic stability, excitations enter the differential equation coefficients and the equations are homogeneous [28]. Saffari et al. [29] analyzed the dynamic stability of FG nanobeam using nonlocal beam theory. According to this study, increasing surface stress makes nanobeam more stable. Talimiyan and Beda [30] investigated the dynamic stability of a size-dependent microbeam. The results show that microbeam in classical theories is more stable than nonlocal theories. There are many mathematical methods for analyzing dynamic stability of systems such as Runge-Kutta Method and the incremental harmonic balance method (IHBM) [31]. Among these methods, the IHBM is useful and highly accurate for nonlinear problems with periodic excitation. Therefore, this method is widely used for nonlinear stability analysis. Wang et al. [32] analyzed the vibrations of nonlinear systems using the IHBM. The results show that this method is capable of analyzing the dynamics of these systems. Gao et al. [33] analyzed dynamic stability of Euler-Bernoulli beams using Chebyshev Surrogate Model. The results show that the method proposed in the study can help design useful, optimized beam-type structures more efficiently than other methods.

In this study, dynamic stability of an Euler-Bernoulli FGM nanobeam is analyzed according to the nonlocal elasticity theory with a sequence of nanoparticle moving over the beam. The properties of FGM nanobeam including Young's Modulus, density and surface residual stress are taken into account as power law. Nanobeam dynamic stability is analyzed linearly and equations of motion are obtained by applying the Hamilton's principle and according to the energy method. The nonlocal equation of motion can be obtained by combining classical equations with the nonlocal elasticity theory and the Gurtin-Murdoch continuum theory. After extracting the governing equations, dynamic stability of nanobeam is analyzed using the incremental harmonic balance method. According to knowledge of authors, the nanobeam dynamic instability region (DIR) is drawn in the dimensionless mass-velocity diagram, for the first time in this paper. This diagram clearly shows the mass and velocity impact of moving nanoparticle in the DIRs of the nanobeam.

2- Governing Equation of motion for an Euler-Bernoulli nanobeam

According to Fig. 1, the nanobeam made from functionally graded material will be assumed to have a length of L, the width of b, and the thickness of h. Nanobeam will be in a Pasternak environment with the Winker elasticity constant of K_W and the shearing constant of K_G. Nanoparticles with a mass of m and the velocity of U are moving over the nanobeam continuously.

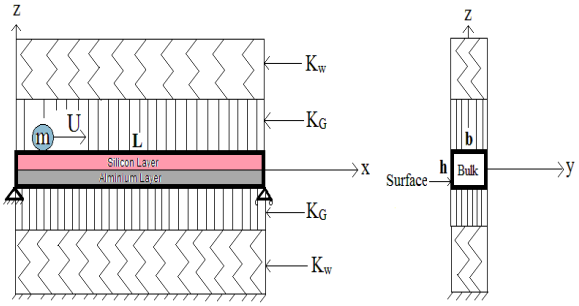

Fig. 1 FG nanobeam in a Pasternak Foundation

According to the power law, the properties of the functionally graded material are as follows [34].

$$E(z)=\left(E_c-E_m\right)\left(\frac{z}{h}+\frac{1}{2}\right)^N+E_m \quad (1)$$

$$\rho(z)=\left(\rho_c-\rho_m\right)\left(\frac{z}{h}+\frac{1}{2}\right)^N+\rho_m \quad (2)$$

$$G(z)=(G_c-G_m)\left(\frac{z}{h}+\frac{1}{2}\right)^N+G_m \quad (3)$$

$$\tau^S(z)=(\tau_c^S-\tau_m^S)\left(\frac{z}{h}+\frac{1}{2}\right)^N+\tau_m^S \quad (4)$$

$$E^S(z)=(E_c^S-E_m^S)\left(\frac{z}{h}+\frac{1}{2}\right)^N+E_m^S \quad (5)$$

$$\alpha_x(z)=(\alpha_{xc}-\alpha_{xm})\left(\frac{z}{h}+\frac{1}{2}\right)^N+\alpha_{xm} \quad (6)$$

$$\alpha_x^S(z)=(\alpha_{xc}^S-\alpha_{xm}^S)\left(\frac{z}{h}+\frac{1}{2}\right)^N+\alpha_{xm}^S \quad (7)$$

The above equations represent elasticity modulus, density, shearing modulus, residual surface stress, surface elasticity modulus, thermal expansion coefficient and the surface thermal expansion coefficient, respectively. The subscript c represents the ceramic section of the FGM nanobeam and the subscript m represents its metal component. N indicates the volume fraction gradient index, which determines the profile variation of material properties across the FG nanobeam thickness. The displacement field for the FG nanobeam on the x, y, and z axis is shown according to the Euler-Bernoulli beam Theory as follows [35]

$$U_x(x,z,t)=u(x,t)-z\frac{\partial w(x,t)}{\partial x} \quad (8a)$$

$$U_y(x,z,t)=0 \quad (8b)$$

$$U_z(x,z,t)=w(x,t) \quad (8c)$$

where $u(x,t)$ and $w(x,t)$ are the displacement coordinates of the nanobeam middle surface in the x and z axis. The linear form of the strain displacement equation is assumed as in Eq. (9) in which ε_{xx} is the axial strain of the functionally graded material nanobeam [35].

$$\varepsilon_{xx}=\frac{\partial u(x,t)}{\partial x}-z\frac{\partial^2 w(x,t)}{\partial^2 x} \quad (9)$$

The force resulting from the thermal gradient will be as follows

$$\overline{N_T}=E(z)A\alpha_x(z)T \quad (10)$$

where $\overline{N_T}$ is the axial force due to the influence of temperature changes, T is the temperature changes, υ is Poisson's ratio and A is nanobeam cross section. The stress field for the bulk of nanobeam is as

$$\sigma_{xx}=E(z)\left(\varepsilon_{xx}-\alpha_x(z)T\right)+\upsilon\sigma_{zz} \quad (11a)$$

$$\sigma_{xz} = 0 \tag{11b}$$

where σ_{zz} can be considered as follows

$$\sigma_{zz} = f(z)\begin{pmatrix} \frac{1}{2}\left(\rho_c^s+\rho_m^s\right)\frac{\partial^2 w}{\partial t^2} \\ -\frac{1}{2}\left(\tau_c^s-\tau_m^s\right)\frac{\partial^2 w}{\partial x^2} \end{pmatrix} \tag{12a}$$

$$f(z) = 2\left(\frac{z}{h}\right)\left[\left(\frac{z}{h}\right)^2 - \frac{3}{4}\right] \tag{12b}$$

According to the Gurtin-Murdoch theory [36], the stress field of surface layers is shown in Eq. (13).

$$\sigma_{xx}^S = E^S(z)\varepsilon_{xx} + \tau^S(z) \tag{13a}$$

$$\sigma_{xz}^S = \tau^S(z)\frac{\partial w}{\partial x} \tag{13b}$$

wher S superscript represents the parameters related to the nanobeam surface. ρ^S and τ^S represent the surface density and surface residual stress, respectively.

2-1 Energy of system

In this section, the energies of system's components will be calculated. All energies in the FG nanobeam structure is taken into account, including the nanobeam strain and kinetic energies, the kinetic and potential energies of nanoparticle and the energy created by the Pasternak foundation. The strain energy and its variable form in the FG nanobeam are as Eq. (14) and Eq. (15), respectively.

$$V_C = \frac{1}{2}\int_0^L \int_{-\frac{h}{2}}^{\frac{h}{2}} \sigma_{xx}\varepsilon_{xx}\,dxdA \tag{14}$$

$$\delta V_C = -\int_0^L \begin{pmatrix} \frac{\partial N}{\partial x}\delta u + \frac{\partial}{\partial x}\left(N\frac{\partial w}{\partial x}\right)\delta w \\ +\frac{\partial^2 M}{\partial x^2}\delta w \end{pmatrix} dx \tag{15}$$

$$N = \int_A \sigma_{xx}\,dA,\ M = \int_A z\sigma_{xx}\,dA. \tag{16}$$

N and M are the FG nanobeam axial force and bending torque. The Euler-Bernoulli beam kinetic energy and its variable form are calculated in Eqs. (18) and (19).

$$\overrightarrow{V_b} = \dot{\vec{r}} = \left(\frac{\partial u}{\partial t} - z\frac{\partial^2 w}{\partial x \partial t}\right)\hat{i} + \frac{\partial w}{\partial t}\hat{k} \tag{17}$$

$$K = \frac{\rho(z)}{2}\int_A \int_0^L \begin{pmatrix} \left(\frac{\partial u}{\partial t} - z\frac{\partial^2 w}{\partial x \partial t}\right)^2 \\ +\left(\frac{\partial w}{\partial t}\right)^2 \end{pmatrix} dxdA \tag{18}$$

$$\int_0^t \delta K dt = \int_0^t \int_0^L \begin{pmatrix} -bI_0\frac{\partial^2 u}{\partial t^2}\delta u \\ +bI_1\frac{\partial^3 w}{\partial x \partial t^2}\delta u \\ -bI_1\frac{\partial^3 u}{\partial x \partial t^2}\delta w \\ +bI_2\frac{\partial^4 w}{\partial x^2 \partial t^2}\delta w \\ -bI_0\frac{\partial^2 w}{\partial t^2}\delta w \end{pmatrix} dxdt. \tag{19}$$

where $\overrightarrow{V_b}$ in Eq. (17) is the velocity field of the nanobeam and I_0, I_1, I_2 are as follows

$$I_0 = \int_{-h/2}^{h/2} \rho(z)dz,\ I_1 = \int_{-h/2}^{h/2} z\rho(z)dz,\ I_2 = \int_{-h/2}^{h/2} z^2\rho(z)dz. \tag{20}$$

The energy created by the Pasternak foundation and its variable form are calculated as follows [12].

$$V = \frac{1}{2}\int_0^L -F_m w b dx, \tag{21}$$

$$F_m = K_W w - K_G\frac{\partial^2 w}{\partial x^2}, \tag{22}$$

$$\delta V = -\int_0^L F_m \delta w b dx. \tag{23}$$

The potential energy of nanoparticles over the Euler-Bernoulli functionally graded nanobeam is shown in Eq. (24).

$$PE_{mass} = mgw\big|_{x=Ut} \tag{24}$$

$$\int_{t_1}^{t_2} \delta PE_{mass}\, dt = \int_{t_1}^{t_2}\int_{0}^{L} mg\,\delta w\,\bar{\delta}(x-Ut)\,dx\,dt \tag{25}$$

In Eq. (25), g is the earth's gravitational acceleration and $\bar{\delta}(x-Ut)$ is the Dirac delta function. The kinetic energy of the nanoparticle passing over the nanobeam is shown in Eq. (26).

$$\int_{t_1}^{t_2} \delta KE_{mass}\, dt = -\int_{t}^{t_2} \left[C\delta u + D\delta w\right]_{x=Ut}\, dt \tag{26}$$

$$C = m\frac{\partial^2 u}{\partial t^2} - mU\frac{\partial^2 u}{\partial x \partial t} \tag{27}$$

$$D = m\frac{\partial^2 w}{\partial t^2} + mU^2\frac{\partial^2 w}{\partial x^2} + 2mU\frac{\partial^2 w}{\partial x \partial t} \tag{28}$$

2-2 Hamilton's principle

According to the Hamilton's principle [37], the total energy variation in the entire period is zero. The equations of motion will be obtained using the Hamilton's principle according to the Eq. (29).

$$\int_{t_1}^{t_2} \delta L\, dt = 0 \tag{29}$$

$$\int_{t_1}^{t_2} \begin{pmatrix} \delta K + \delta KE_{mass} - \delta V \\ -\delta PE_{mass} - \delta V_c \end{pmatrix} dt = 0. \tag{30}$$

By replacing the coefficients of δu and δw in Eq. (30) with zeros, classical equations of motion will be obtained as follows

$$\begin{aligned} &\frac{\partial N}{\partial x} - bI_0\frac{\partial^2 u}{\partial t^2} + bI_1\frac{\partial^3 w}{\partial x \partial t^2} \\ &- m\frac{\partial^2 u}{\partial t^2}\bigg|_{x=Ut} + mU\frac{\partial^2 u}{\partial x \partial t}\bigg|_{x=Ut} = 0 \end{aligned} \tag{31}$$

$$\begin{aligned} &\frac{\partial^2 M}{\partial x^2} + \frac{\partial}{\partial x}\left(N\frac{\partial w}{\partial x}\right) - bI_1\frac{\partial^3 u}{\partial x \partial t^2} \\ &+ bI_2\frac{\partial^4 w}{\partial x^2 \partial t^2} - bI_0\frac{\partial^2 w}{\partial t^2} - m\frac{\partial^2 w}{\partial t^2}\bigg|_{x=Ut} \\ &- mU^2\frac{\partial^2 w}{\partial x^2}\bigg|_{x=Ut} - 2mU\frac{\partial^2 w}{\partial x \partial t}\bigg|_{x=Ut} \\ &+ bF_m - mg\bar{\delta}(x-Ut) = 0 \end{aligned} \tag{32}$$

2-3 Axial force and bending torque of FG nanobeam

The FG nanobeam axial force for bulk and surface is as follows

$$N_{xx}^{l} = \int_{-\frac{h}{2}}^{\frac{h}{2}} \sigma_{xx} b\, dz + \oint_{\Gamma} \sigma^s ds. \tag{33}$$

Replacing Eq. (11) and (13) into Eq. (33) will lead to

$$\begin{aligned} N_{xx}^{l} &= A_{11} b\frac{\partial u}{\partial x} + \frac{1}{2}A_{11} b\left(\frac{\partial w}{\partial x}\right)^2 \\ &- B_{11} b\frac{\partial^2 w}{\partial x^2} - T_{11} bT + \\ &+ A_s\frac{\partial u}{\partial x} + A_s\frac{1}{2}\left(\frac{\partial w}{\partial x}\right)^2 \\ &- B_s\frac{\partial^2 w}{\partial x^2} + M_s - T_s T \end{aligned} \tag{34}$$

Also the bending torque of the FGM nanobeam for the bulk and surface is according to Eq. (35).

$$M_{xx}^{l} = \int_{-\frac{h}{2}}^{\frac{h}{2}} z\,\sigma_{xx} b\, dz + \oint_{\Gamma} z\,\sigma^s ds. \tag{35}$$

Replacing Eq. (11) and Eq. (13) will simplify Eq. (35) as follows

$$
\begin{aligned}
M_{xx}^{l} &= B_{11}b\frac{\partial u}{\partial x}+\frac{1}{2}B_{11}b\left(\frac{\partial w}{\partial x}\right)^2 \\
&- D_{11}b\frac{\partial^2 w}{\partial x^2}-R_{11}bT-\frac{1}{10}h^2\upsilon Yb \\
&+ B_s\frac{\partial u}{\partial x}+B_s\frac{1}{2}\left(\frac{\partial w}{\partial x}\right)^2 \\
&- D_s\frac{\partial^2 w}{\partial x^2}+N_s-R_sT
\end{aligned}
\tag{36}
$$

where in Eq. (34) and Eq. (36) bellow parameters are define

$$
\left[A_{11},B_{11},D_{11}\right]=\int_{-\frac{h}{2}}^{\frac{h}{2}}E(z)\left[1,z,z^2\right]dz,
\tag{37}
$$

$$
\left[A_s,B_s,D_s\right]=\oint_{\Gamma}E^s(z)\left[1,z,z^2\right]ds,
$$

$$
\left[M_s,N_s\right]=\oint_{\Gamma}\tau^s(z)\left[1,z\right]ds,
\tag{38}
$$

$$
\left[T_{11},R_{11}\right]=\int_{-\frac{h}{2}}^{\frac{h}{2}}E(z)\alpha_x(z)\left[1,z\right]dz
$$

$$
\left[T_s,R_s\right]=\oint_{\Gamma}E^s(z)\alpha_x(z)\left[1,z\right]ds.
\tag{39}
$$

2-4 Nonlocal elasticity theory

According to Eringen nonlocal elasticity theory, the stress equation is as follows [2].

$$
\left(1-\mu^2\frac{\partial^2}{\partial x^2}\right)\sigma_{ij}^{nl}=\sigma_{ij}^{l}
\tag{40}
$$

where $\mu=e_0a$ is the small scale effect, e_0 is the non-dimensional parameter for each material and a is the internal characteristic length. Also σ_{ij}^{l} and σ_{ij}^{nl} are the local and nonlocal stress tensors. The first and second equations governing the nonlocal Euler-Bernoulli FG nanobeam result in Eqs. (41, 42).

$$
\begin{aligned}
&\left(A_{11}b+A_s\right)\left(\frac{\partial^2 u}{\partial x^2}+\frac{1}{2}\frac{\partial}{\partial x}\left(\frac{\partial w}{\partial x}\right)^2\right) \\
&-\left(B_{11}b+B_s\right)\frac{\partial^3 w}{\partial x^3}-\frac{\partial}{\partial x}T_{11}bT+\frac{\partial}{\partial x}M_s \\
&+\mu^2\begin{pmatrix} bI_0\dfrac{\partial^4 u}{\partial x^2\partial t^2}-bI_1\dfrac{\partial^5 w}{\partial x^3\partial t^2} \\ +m\left(\dfrac{\partial^4 u}{\partial x^2\partial t^2}-U\dfrac{\partial^4 u}{\partial x^3\partial t}\right)_{x=Ut}\end{pmatrix} \\
&-\frac{\partial}{\partial x}T_sT \quad =bI_0\frac{\partial^2 u}{\partial t^2}-bI_1\frac{\partial^3 w}{\partial x\partial t^2} \\
&+m\left(\frac{\partial^2 u}{\partial t^2}-U\frac{\partial^2 u}{\partial x\partial t}\right)_{x=Ut},
\end{aligned}
\tag{41}
$$

$$
\begin{aligned}
&(B_{11}b+B_s)\left(\frac{\partial^3 u}{\partial x^3}+\frac{1}{2}\frac{\partial^2}{\partial x^2}\left(\frac{\partial w}{\partial x}\right)^2\right) \\
&-\left(D_{11}b+D_s\right)\frac{\partial^4 w}{\partial x^4}-\frac{\partial^2}{\partial x^2}R_{11}bT \\
&-\frac{\partial^2}{\partial x^2}\frac{\upsilon Ybh^2}{10}+\frac{\partial^2}{\partial x^2}N_s-\frac{\partial^2}{\partial x^2}R_sT \\
&+\mu^2\left[-\left(\frac{\partial^3 N}{\partial x^3}\frac{\partial w}{\partial x}+\frac{\partial N}{\partial x}\frac{\partial^3 w}{\partial x^3}+\frac{\partial^2 N}{\partial x^2}\frac{\partial^2 w}{\partial x^2}\right)\right] \\
&+\mu^2\left[-\begin{pmatrix} N\dfrac{\partial^4 w}{\partial x^4}-bI_1\dfrac{\partial^5 u}{\partial x^3\partial t^2}+bI_2\dfrac{\partial^6 w}{\partial x^4\partial t^2} \\ -bI_0\dfrac{\partial^4 w}{\partial x^2\partial t^2}\end{pmatrix}\right] \\
&+\mu^2\left[\begin{matrix} +m\left(\dfrac{\partial^4 w}{\partial x^2\partial t^2}+U^2\dfrac{\partial^4 w}{\partial x^4}+2U\dfrac{\partial^4 w}{\partial x^3\partial t}\right) \\ -b\left(k_w\dfrac{\partial^2 w}{\partial x^2}-k_G\dfrac{\partial^4 w}{\partial x^4}\right)\end{matrix}\right] \\
&+\mu^2\left[+mg\frac{\partial^2}{\partial x^2}\bar{\delta}(x-Ut)\right]=-\frac{\partial}{\partial x}\left(N\frac{\partial w}{\partial x}\right) \\
&+bI_1\frac{\partial^3 u}{\partial x\partial t^2}-bI_2\frac{\partial^4 w}{\partial x^2\partial t^2}+bI_0\frac{\partial^2 w}{\partial t^2} \\
&+m\left(\frac{\partial^2 w}{\partial t^2}+U^2\frac{\partial^2 w}{\partial x^2}+2U\frac{\partial^2 w}{\partial x\partial t}\right)_{x=Ut} \\
&-b\left(k_w w-k_G\frac{\partial^2 w}{\partial x^2}\right)+mg\bar{\delta}(x-Ut).
\end{aligned}
\tag{42}
$$

Using the Galerkin method for simply supported nanobeam as

$$u(x,t)=u(t)\sin\left(\frac{\pi x}{L}\right),\ w(x,t)=w(t)\sin\left(\frac{\pi x}{L}\right)$$

and the non-dimensional groups of Eq. (43), the dimensionless equations can be obtained.

$$\begin{aligned}
&\tau=\frac{t\pi U}{L},u(\tau)=\frac{u(\mathrm{t})}{L},\ w(\tau)=\frac{w(\mathrm{t})}{h},\\
&\lambda=\frac{\mu}{L},\varphi=\sqrt{\frac{U^2 I_0}{hE_m}},M=\frac{m}{L^2\mathrm{I}_0},\\
&\overline{\mathrm{A}_{11}}=\frac{\mathrm{A}_{11}}{\mathrm{E}_c h},\zeta=\frac{b}{L},\overline{\mathrm{A}_S}=\frac{\mathrm{A}_S}{\mathrm{E}_c hL},\\
&\overline{\mathrm{I}_1}=\frac{\mathrm{I}_1}{L\mathrm{I}_0},\gamma=\frac{h}{L},\overline{B_S}=\frac{B_S}{\mathrm{E}_c L^3},\overline{E}=\frac{E_m}{\mathrm{E}_c},\\
&\overline{B_{11}}=\frac{B_{11}}{\mathrm{E}_c L^2},\overline{\mathrm{T}_{11}}=\frac{\mathrm{T}_{11}T}{\mathrm{E}_c L},\overline{T_S}=\frac{T_S T}{\mathrm{E}_c L^2},\\
&\overline{D_{11}}=\frac{D_{11}}{\mathrm{E}_c L^3},\overline{I_2}=\frac{I_2}{L^2 I_0},\overline{M_S}=\frac{M_S}{\mathrm{E}_c L^2}\\
&,\overline{\mathrm{k}_g}=\frac{\mathrm{k}_g}{\mathrm{E}_c L},\overline{D_S}=\frac{D_S}{\mathrm{E}_c L^4},\overline{k_W}=\frac{k_W L}{\mathrm{E}_c},\\
&\overline{\rho_m^s}=\frac{\rho_m^s}{I_0},\overline{\rho_c^s}=\frac{\rho_c^s}{I_0},\overline{\tau_m^s}=\frac{\tau_m^s}{\mathrm{E}_c L},\overline{\tau_c^s}=\frac{\tau_c^s}{\mathrm{E}_c L}.
\end{aligned}\tag{43}$$

3- Solution Method

The incremental harmonic balance method is highly accurate in finding periodic solutions including dynamic stability analysis. In this method (M^*,φ^*) is considered to be a known point on the instability boundary. In order to determine other points on the boundary of instability, an increment is assigned to the specific point to find the point neighboring the boundary of instability. Therefore, points on the instability boundary are determined and the stable regions are distinguished from instable ones. The IHBM algorithm is given in Fig. 2.

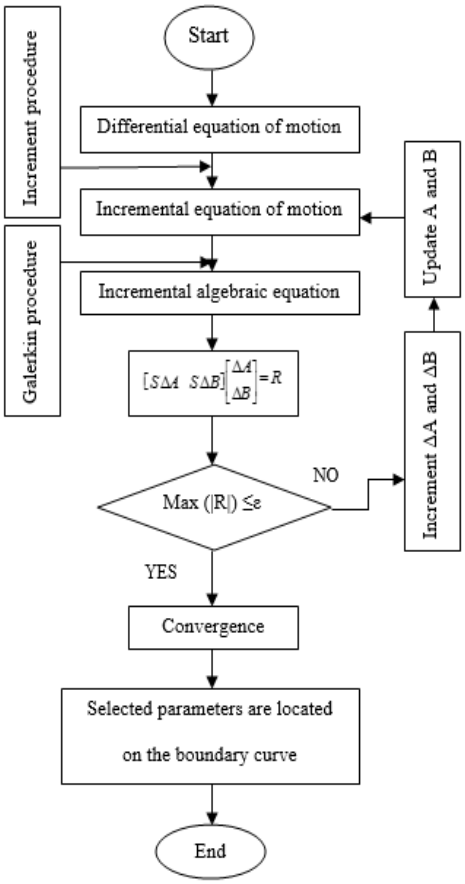

Fig. 2 Incremental Harmonic Balance Method algorithm

4- Results and Discussion

The nanobeam length is equal to 13*nm* and its width and thickness is equal to one tenth of its length. The thermal expansion coefficient is $\alpha_x=-1.6\times10^{-6}\left(1/^\circ K\right)$. The Pasternak shearing constant is $k_G=2.071273\left(N/m\right)$, the Winkler elasticity coefficient is $k_W=8.9995035\times10^{17}\left(N/m^3\right)$ and the nonlocal small scale parameter is $e_0a=1\left(nm\right)$. The functionally graded nanobeam properties are given in Table 1.

Table 1: Properties of FG nanobeam

Material	Aluminum	Silicon
$E(Gpa)$	70	210
$E^S(N/m)$	5.1882	-10.6543
υ	0.3	0.24
$\rho(kg/m^3)$	2800	2370
$\tau^S(N/m)$	0.9108	0.6048
$\rho^S(kg/m^2)$	5.46e-7	3.17e-7

Fig. 3 shows the DIRs of FG nanobeam for solutions corresponding to the T and 2T periods. Instable regions are obtained using the Fourier series function, respectively for the T and 2T periods.

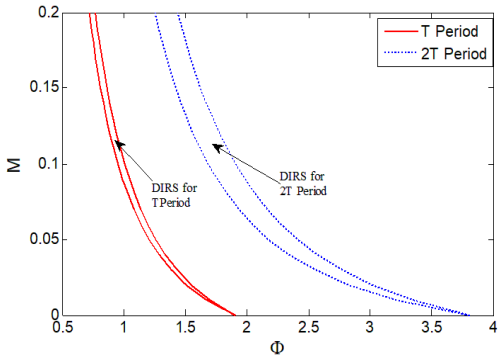

Fig. 3 DIRs of FG nanobeam for T and 2T periods

As seen in Fig. 3, the instable regions obtained using the IHBM determine the boundary regions of stability and instability. As seen in Fig. 3 there is an instable region between each tab. All Euler-Bernoulli FG nanobeam dynamic stability graphs are drawn on the non-dimensional mass-velocity coordinates. Comparing the instable regions of the T and 2T periods shows that, since the DIRs in the T period has occurred in lower velocity, the FG nanobeam is more instable in the T period than in the 2T period. Also width of DIRs in the T period is smaller than 2T period.

Considering that nanobeam dynamic stability is nowhere to be seen on the non-dimensional mass-velocity graphs of previous studies, the time response of first mode vibration for one of the points inside the DIRs in Fig. 4.(a) has been drawn according to the Runge-Kutta method in order to validate the results. As seen at point $M=0.15,\varphi=0.8$ which has been chosen from the DIRs of the nanobeam in the T period, the curve diverges, which indicates the instability of this region. Also with regards to the dynamic stability point $M=0.15,\varphi=0.84$ in the T period, the periodic response graph drawn in Fig. 4.(b) shows that this point in the system is dynamically stable.

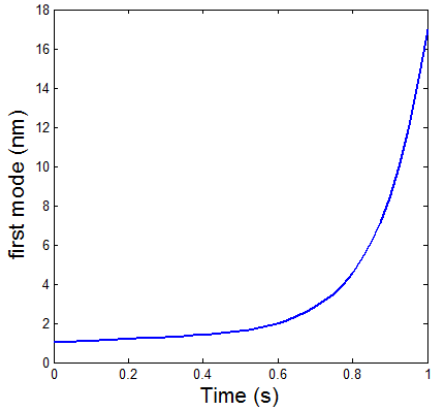

4 (a)

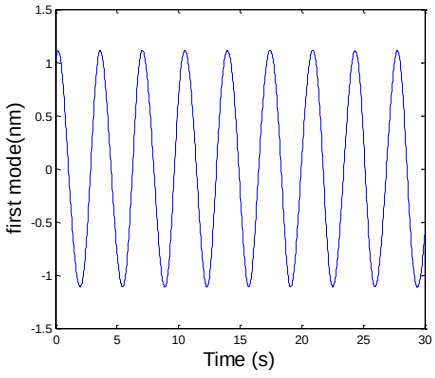

4 (b)

Fig. 4 (a) $M=0.15,\varphi=0.8$ is instable point and (b) $M=0.15,\varphi=0.84$ is stable point in DIRs of FG nanobeam.

Fig. 5. shows the small scale effect parameter on instable regions of the nanobeam in the T and 2T periods. As seen in the dynamic stability graph, increasing this parameter causes the DIRs of FG nanobeam to shift towards slower nanoparticles. Therefore, the FG nanobeam becomes more unstable by increasing the small scale parameter. By increasing this parameter, which represents the bond length between atoms, the nanobeam hardness decreases and causes it to quickly become instable. The mass and velocity for small scale parameter variation in the T and 2T periods are given in Table 2.

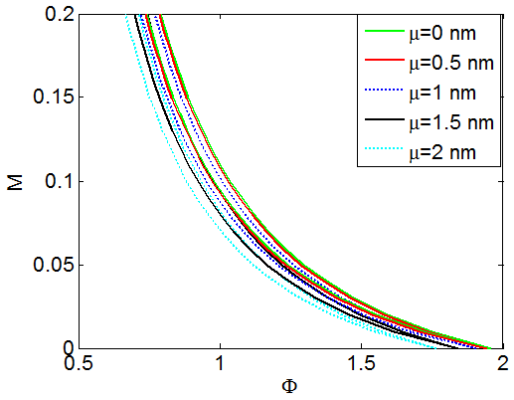

5(a)

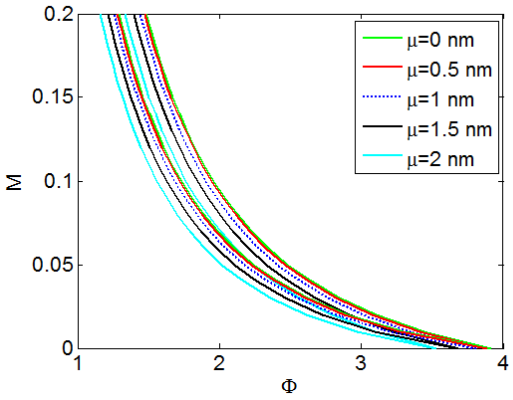

5 (b)

Fig. 5 Effect of small scale parameter on DIRs of FG nanobeam for (a) T period and (b) 2T period.

Table 2: The non-dimensional mass and velocity for small scale parameter variation in the **(a)** T and **(b)** 2T periods

$M = 0.1$	φ (First branch)	φ (Second branch)
$\mu = 0nm$	0.9806	0.037
$\mu = 0.5nm$	0.9735	1.029
$\mu = 1nm$	0.953	1.008
$\mu = 1.5nm$	0.9219	0.9136
$\mu = 2nm$	0.8829	0.933

(a)

$M = 0.1$	φ (First branch)	φ (Second branch)
$\mu = 0nm$	1.733	1.961
$\mu = 0.5nm$	1.72	1.947
$\mu = 1nm$	1.684	1.906
$\mu = 1.5nm$	1.629	1.844
$\mu = 2nm$	1.559	1.766

(b)

Fig. 6 shows the effect of Pasternak shearing constant on instable regions. As expected, increasing the Pasternak shearing constant makes the FG nanobeam more stable and the DIRs shifts towards faster velocity. The elastic environments increasing hardness in this conditions, which limits the scope of beam's movement, makes it more stable.

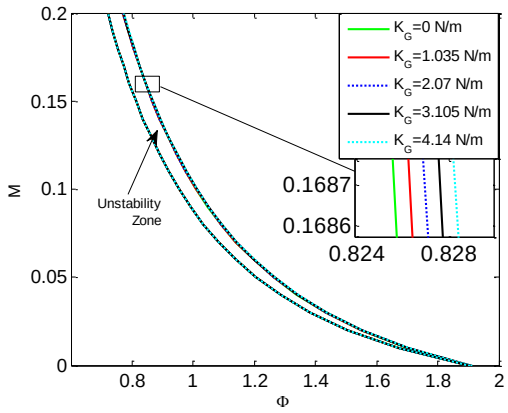

Fig. 6 Effect of the Pasternak shearing constant on DIRs of FG nanobeam

Fig. 7 shows the effect of the Winkler elasticity constant on unstable region. Increasing the Winkler elasticity constant makes the FG nanobeam more stable and the DIRs of nanobeam shift towards faster velocity of nanoparticles.

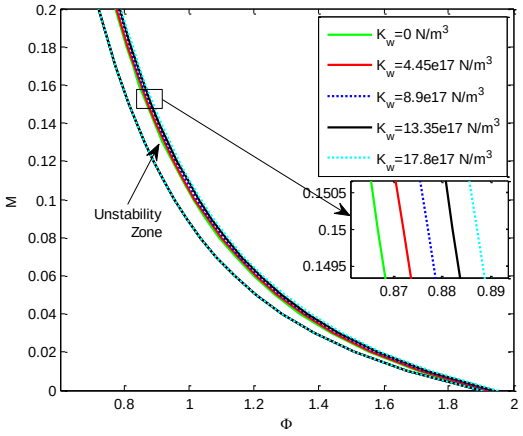

Fig. 7 Effect of the Winkler elasticity constant on DIRs of FG nanobeam

Fig. 8 shows the effect of temperature variation on the FG nanobeam DIRs in low temperature conditions. Despite the stress put on the FG nanobeam, the thermal gradient on the nanobeam is assumed to have constant temperature changes. This graph shows that increasing temperature makes the nanobeam shifts towards further stability. In other words, the FG Euler-Bernoulli nanobeam has become more stable with increased temperature. The results of the dynamic stability analysis of the Euler-Bernoulli FG nanobeam using the power law to approximate the behavior of the FGM also shows that increasing the volume fraction parameter has made the nanobeam instable. Fig. 9 shows the effect of variations in the volume fraction power parameter *N* in the power law. Increasing this parameter shifts the area of instability towards lower speeds and the FG nanobeam become less stable.

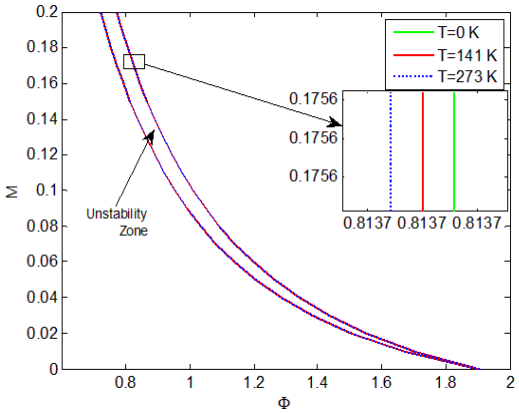

Fig. 8 Effect of temperature variation on the FGM nanobeam DIRs

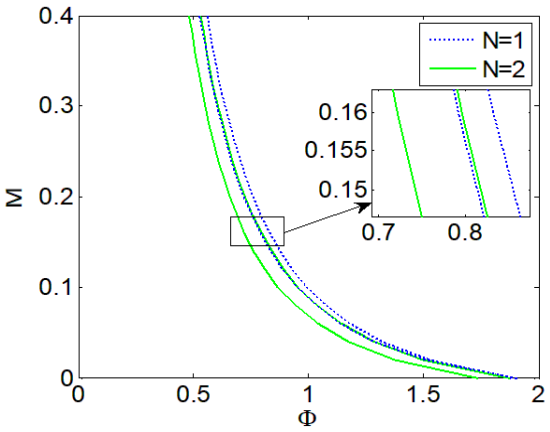

Fig. 9 Effect of variations in the volume fraction power parameter N in the power law

5- Conclusion

In this study, the dynamic stability of the Euler-Bernoulli FGM nanobeam with continuum nanoparticles passing over was investigated while taking surface effects into account, according to the nonlocal

elasticity theory. The nanobeam supports are normal and it is inn Pasternak foundation. Dynamic instability boundaries are plotted and instability points are marked. The results of this study showed that the instability tab for the T periods occurred at lower speeds than the instability tab in 2T periods. Also, the instability tab in T periods is more closed than 2T periods. So more points are unstable during the 2T periods. Also, the nanobeam exhibits higher stability by increasing the Pasternak foundation hardness. This stiffness includes Pasternak shear constant and Winkler spring constant. Increasing temperature also makes the FGM nanobeam less stable and the DIRs tab in the mass-velocity diagram shifts towards lower velocity. With increasing small-scale parameter and inter-atomic bonds, nanobeam has become more unstable. The results of this research can be used in the design of NEMS and targeted drug injection systems.

References

[1] Mindlin, R. D. (1965). Second gradient of strain and surface-tension in linear elasticity. *International Journal of Solids and Structures*, *1*(4), 417-438.

[2] Eringen, A. C. (2006). Nonlocal continuum mechanics based on distributions. *International Journal of Engineering Science*, *44*(3-4), 141-147.

[3] Lu, L., Guo, X., & Zhao, J. (2017). A unified nonlocal strain gradient model for nanobeams and the importance of higher order terms. *International Journal of Engineering Science*, *119*, 265-277.

[4] Peddieson, J., Buchanan, G. R., & McNitt, R. P. (2003). Application of nonlocal continuum models to nanotechnology. *International journal of engineering science*, *41*(3-5), 305-312.

[5] Ansari, R., & Sahmani, S. (2011). Bending behavior and buckling of nanobeams including surface stress effects corresponding to different beam theories. *International Journal of Engineering Science*, *49*(11), 1244-1255.

[6] Ashoori, A. R., Salari, E., & Vanini, S. S. (2016). Size-dependent thermal stability analysis of embedded functionally graded annular nanoplates based on the nonlocal elasticity theory. *International Journal of Mechanical Sciences*, *119*, 396-411.

[7] Atabakhshian, V., Shooshtari, A., & Karimi, M. (2015). Electro-thermal vibration of a smart coupled nanobeam system with an internal flow based on nonlocal elasticity theory. *Physica B: Condensed Matter*, *456*, 375-382.

[8] Bağdatli, S. M., & Togun, N. (2017). Stability of fluid conveying nanobeam considering nonlocal elasticity. *International Journal of Non-Linear Mechanics*, *95*, 132-142.

[9] Hashemi, S. H., & Khaniki, H. B. (2018). Dynamic response of multiple nanobeam system under a moving nanoparticle. *Alexandria engineering journal*, *57*(1), 343-356.

[10] Şimşek, M. (2010). Vibration analysis of a single-walled carbon nanotube under action of a moving harmonic load based on nonlocal elasticity theory. *Physica E: Low-dimensional Systems and Nanostructures*, *43*(1), 182-191.

[11] Kiani, K., & Mehri, B. (2010). Assessment of nanotube structures under a moving nanoparticle using

nonlocal beam theories. *Journal of Sound and Vibration*, *329*(11), 2241-2264.

[12] Arani, A. G., & Roudbari, M. A. (2013). Nonlocal piezoelastic surface effect on the vibration of visco-Pasternak coupled boron nitride nanotube system under a moving nanoparticle. *Thin Solid Films*, *542*, 232-241.

[13] Kiani, K. (2011). Small-scale effect on the vibration of thin nanoplates subjected to a moving nanoparticle via nonlocal continuum theory. *Journal of Sound and Vibration*, *330*(20), 4896-4914.

[14] Li, Y. H., Wang, L., & Yang, E. C. (2018). Nonlinear dynamic responses of an axially moving laminated beam subjected to both blast and thermal loads. *International Journal of Non-Linear Mechanics*, *101*, 56-67.

[15] Şimşek, M. (2010). Non-linear vibration analysis of a functionally graded Timoshenko beam under action of a moving harmonic load. *Composite Structures*, *92*(10), 2532-2546.

[16] Chang, T. P. (2013). Stochastic FEM on nonlinear vibration of fluid-loaded double-walled carbon nanotubes subjected to a moving load based on nonlocal elasticity theory. *Composites Part B: Engineering*, *54*, 391-399.

[17] Liu, J. J., Li, C., Fan, X. L., & Tong, L. H. (2017). Transverse free vibration and stability of axially moving nanoplates based on nonlocal elasticity theory. *Applied Mathematical Modelling*, *45*, 65-84.

[18] Rahmani, O., Niaei, A. M., Hosseini, S. A. H., & Shojaei, M. (2017). In-plane vibration of FG micro/nano-mass sensor based on nonlocal theory under various thermal loading via differential transformation method. *Superlattices and Microstructures*, *101*, 23-39.

[19] Sedighi, H. M., Keivani, M., & Abadyan, M. (2015). Modified continuum model for stability analysis of asymmetric FGM double-sided NEMS: corrections due to finite conductivity, surface energy and nonlocal effect. *Composites Part B: Engineering*, *83*, 117-133.

[20] Eltaher, M. A., Khairy, A., Sadoun, A. M., & Omar, F. A. (2014). Static and buckling analysis of functionally graded Timoshenko nanobeams. *Applied Mathematics and Computation*, *229*, 283-295.

[21] Vafakhah, Z., & Neya, B. N. (2019). An exact three dimensional solution for bending of thick rectangular FGM plate. *Composites Part B: Engineering*, *156*, 72-87.

[22] Hosseini-Hashemi, S., & Nazemnezhad, R. (2013). An analytical study on the nonlinear free vibration of functionally graded nanobeams incorporating surface effects. *Composites Part B: Engineering*, *52*, 199-206.

[23] Hosseini-Hashemi, S., Nazemnezhad, R., & Bedroud, M. (2014). Surface effects on nonlinear free vibration of functionally graded nanobeams usi

[24] Ke, L. L., & Wang, Y. S. (2011). Size effect on dynamic stability of functionally graded microbeams based on a modified couple stress theory. *Composite Structures*, *93*(2), 342-350.

[25] Rahmani, O., & Pedram, O. (2014). Analysis and modeling the size effect on vibration of functionally graded

nanobeams based on nonlocal Timoshenko beam theory. *International Journal of Engineering Science*, *77*, 55-70.

[26] Pei, Y. L., Geng, P. S., & Li, L. (2018). A modified higher-order theory for FG beams. *European Journal of Mechanics-A/Solids*, *72*, 186-197.

[27] Yang, J., Ke, L. L., & Kitipornchai, S. (2010). Nonlinear free vibration of single-walled carbon nanotubes using nonlocal Timoshenko beam theory. *Physica E: Low-dimensional Systems and Nanostructures*, *42*(5), 1727-1735.

[28] Huang, Y., Fu, J., & Liu, A. (2019). Dynamic instability of Euler–Bernoulli nanobeams subject to parametric excitation. *Composites Part B: Engineering*, *164*, 226-234.

[29] Saffari, S., Hashemian, M., & Toghraie, D. (2017). Dynamic stability of functionally graded nanobeam based on nonlocal Timoshenko theory considering surface effects. *Physica B: Condensed Matter*, *520*, 97-105.

[30] Talimian, A., & Béda, P. (2018). Dynamic stability of a size-dependent micro-beam. *European Journal of Mechanics-A/Solids*, *72*, 245-251.

[31] Kong, X., Sun, W., Wang, B., & Wen, B. (2015). Dynamic and stability analysis of the linear guide with time-varying, piecewise-nonlinear stiffness by multi-term incremental harmonic balance method. *Journal of Sound and Vibration*, *346*, 265-283.

[32] Wang, S., Hua, L., Yang, C., Han, X., & Su, Z. (2019). Applications of incremental harmonic balance method combined with equivalent piecewise linearization on vibrations of nonlinear stiffness systems. *Journal of Sound and Vibration*, *441*, 111-125.

[33] Gao, K., Gao, W., Wu, B., & Song, C. (2019). Nondeterministic dynamic stability assessment of Euler–Bernoulli beams using Chebyshev surrogate model. *Applied Mathematical Modelling*, *66*, 1-25.

[34] Uymaz, B. (2013). Forced vibration analysis of functionally graded beams using nonlocal elasticity. *Composite Structures*, *105*, 227-239.

[35] Fernández-Sáez, J., & Zaera, R. (2017). Vibrations of Bernoulli-Euler beams using the two-phase nonlocal elasticity theory. *International Journal of Engineering Science*, *119*, 232-248.

[36] Gurtin, M. E., & Murdoch, A. I. (1978). Surface stress in solids. *International Journal of Solids and Structures*, *14*(6), 431-440.

[37] Arani, A. G., Hashemian, M., & Kolahchi, R. (2013). Time discretization effect on the nonlinear vibration of embedded SWBNNT conveying viscous fluid. *Composites Part B: Engineering*, *54*, 298-306.